Iranian Journal of Materials Science and Engineering, Vol. 20, Number 3, September 2023
RESEARCH PAPER

The Effect of Boron Reinforced on the Supercapacitor Performance of RGO/ZnO:B Composite Electrodes

Ayça Tanrıverdi[1,2,*] and saniye Tekerek[1,2]

* *aycatanriverdikudret@gmail.com*

[1] Department of Material Science and Engineering, Graduate School of Natural and Applied Sciences, Kahramanmaras¸ Sütcü Imam University, Kahramanmaras, Turkey
[2] Kahramanmaras Sütcü Imam University, Vocational School of Health Services, Dept. of Medical Services and Techniques, Kahramanmaras, Turkey

Received: July 2023 **Revised: August 2023** **Accepted: September 2023**
DOI: 10.22068/ijmse.3306

Abstract: *In this study, zinc chloride ($ZnCl_2$) was used as a precursor chemical to form boron-reinforced zinc oxide (ZnO: B) particles. The supercapacitor performance of the reduced graphene oxide/boron reinforced zinc oxide (RGO/ZnO: B) composite electrodes produced by hydrothermal methods and the impact of different boron doping ratios on the capacitance, were both examined. The characterization of the RGO/ZnO: B composites containing 5%, 10%, 15%, and 20% boron by weight was performed using X-ray diffraction (XRD) and scanning electron microscopy (SEM). The capacitance measurements of the electrodes produced were conducted in a 6 M KOH aqueous solution with a typical three-electrode setup using Iviumstat potentiostat/galvanostatic cyclic voltammetry. The specific capacitance value of the 20% reinforced RGO/ZnO: B composite electrode was 155.88 F/g, while that of the RGO/ZnO composite electrode was 36.37 F/g. According to this result, the capacitance increased four-fold with a 20% boron doping concentration. Moreover, a longer cycle performance was observed for the RGO/ZnO: B electrodes with higher boron doping concentrations.*

Keywords: *RGO/ZnO: B, Boron, composite material, Supercapacitor.*

1. INTRODUCTION

In developing countries, rapid population increase, and industrialization has accelerated energy demand. This increase in energy demand worldwide mandates the development of new energy resources and more efficient use of the storage capacity of the ones already available [1]. In recent years, the increasing popularity of portable electronic devices, and newly produced electric motors and hybrid vehicles has led to an increasing interest in environmentally friendly high-capacity energy storage systems [2-4]. Supercapacitors, which are a type of energy storage device, have advantages such as short charging times, high power density, long cycle life, and low maintenance costs [5–7]. In supercapacitors, the charge-storing event takes place on electrodes. Therefore, most of the studies on supercapacitors have focused on the development of electrode materials and a corresponding increase in power density [8].
Mostly porous carbon-based materials like graphene are used as electrode materials for supercapacitors [9,10]. High-performance nano-composite structures of graphene and graphene-based materials are at the forefront of energy device applications, both in energy production and energy storage [11–19]. Recently, metal oxide composites have attracted great attention in energy transformation and storage applications [20,21]. In supercapacitor applications, graphene metal oxide composite materials have been created to increase the individual properties of graphene and metal oxides [22–26]. Various methods can be utilized to produce these composite materials. For the synthesis of nano-sized metal oxide particles, many different methods using polar and nonpolar solvent systems such as sol-gel [27], hydrolysis of inorganic salts [28], ultrasonic techniques [29], microemulsions [30], and hydrothermal methods [31–33] are available from published literature. Among these methods, hydrothermal synthesis is the most promising method since it allows finer control of the particle size, the crystallinity, and the shape of the nano-sized materials. Hydrothermal synthesis is among the most prevalent methods used to produce nanomaterials and they can be produced over a wide temperature window ranging from room temperature to very high temperatures. Depending on the reaction vapor pressure, low-pressure or high-pressure conditions can be used to influence the

[DOI: 10.22068/ijmse.3306]

morphology of the materials to be synthesized [34]. In this study, RGO/ZnO: B composite materials were produced using the hydrothermal method. The physical characterizations of the fabricated structures were investigated. The effect of boron supplementation on structural change was investigated. Electrochemical performance of Graphite/PTFE/RGO/ZnO:B electrodes were investigated by doping different boron ratios (5, 10, 15, and 20 wt%) to ZnO, and the effect of boron on specific capacitance value was investigated. There are studies in the literature regarding the doping of boron to metal oxide materials at low rates. However, there are not enough studies on the production of supercapacitor electrodes based on high rates of boron supplementation to ZnO. The study aims to contribute to the literature and to shed light on other studies.

2. EXPERIMENTAL PROCEDURES

2.1. Materials

The following raw materials were used for co-precipitation:
Zinc chloride (extra pure, Merck), Hexa-methylenetetramine (for synthesis, Sigma-Aldrich), Boric acid (for analysis, Merck), Graphite powder (<20 μm, synthetic, Sigma Aldrich), Sulfuric acid (95-97%, Merck), Potassium permanganate (cryst, extra pure, Merck), Hydrogen peroxide (30%, Sigma Aldrich), Poly(tetrafluoroethylene) (powder >40μm particle size).

2.2. Preparation of the Graphene Oxide

Graphene oxide (GO) was produced from natural graphite powders using Hummers' method in 3 stages at low, medium, and high temperatures [35–37].
In an ice bath, sulfuric acid (H_2SO_4) was added to 2 g of graphite powder, and the solution was mixed for 30 minutes with a magnetic stirrer. Then 8 g of potassium permanganate ($KMnO_4$) was slowly added to the mixture, during which the solution was always kept below 10˚C by stirring for 2 hours in an ice bath. Later, the solution was placed in a water bath at a temperature of 35˚C and mixed for one hour. The density of the mixture further increased, and 100 mL of ultra-pure water was added dropwise. After that, the solution was kept in a pre-prepared water bath at 98˚C degree for 15 minutes and diluted with 300 mL of ultra-pure water. Later, 20 mL of 30% hydrogen peroxide (H_2O_2) was added to the mixture to completely reduce the $KMnO_4$. The solution was kept at room temperature overnight. To remove the metal ions in the precipitate, it was washed with 800 mL of a 5% hydrochloric acid (HCl) solution. Then, to remove any residual acid, the filtered mixture was washed one last time with 1 L of ultra-pure water.

2.3. Synthesis of the RGO/ZnO: B Composites

Zinc oxide-reinforced boron particles (ZnO: B) were synthesized using the hydrothermal method with zinc chloride ($ZnCl_2$) as a precursor. 0.1M zinc chloride ($ZnCl_2$), 0.1 M boric acid (H_3BO_3), and 0.1M hexamethylene tetramine ($C_6H_{12}N_4$) were dissolved in 100 mL of pure water. To shrink the particle size, ammonia (NH_3) was added dropwise to make the solution pH equal to 10. The solution was put in a Teflon-covered autoclave and kept under 200˚C for 3 hours. The solution was left to cool at room temperature and later ZnO: B particles were filtered from it. The ZnO: B particles were washed with pure water to remove the organic constituents and before the characterization, they were annealed at a temperature of 450˚C for 1 hour.
There are many studies in the published literature on factors such as pH and temperature that affect the morphology and size of the ZnO particles produced [38–40]. In this study, boron was used to dope ZnO in varying weight ratios (5%, 10%, 15%, and 20%) to produce ZnO: B particles. All experimental conditions were held the same for all samples. A tenth of a gram of GO was mixed for 1 hour in an ultrasound mixer in a solution of 20 mL of pure water and 10 mL of ethanol (C_2H_5OH), and then 0.1 g of ZnO: B nanoparticles were added to this GO solution and it was further mixed by ultrasound for 2 hours. The suspension obtained was put in a Teflon-covered autoclave and kept under 160˚C for 3 hours. Thus, the GO was converted to RGO, and ZnO: B particles entering between the RGO layers were chemically bonded to each other, and consequently the composite material RGO/ZnO: B was obtained.
After this composite was filtered and washed with pure water, it was dried at room temperature leaving the synthesized RGO/ZnO: B composite material (Fig. 1).

[DOI: 10.22068/ijmse.3306]

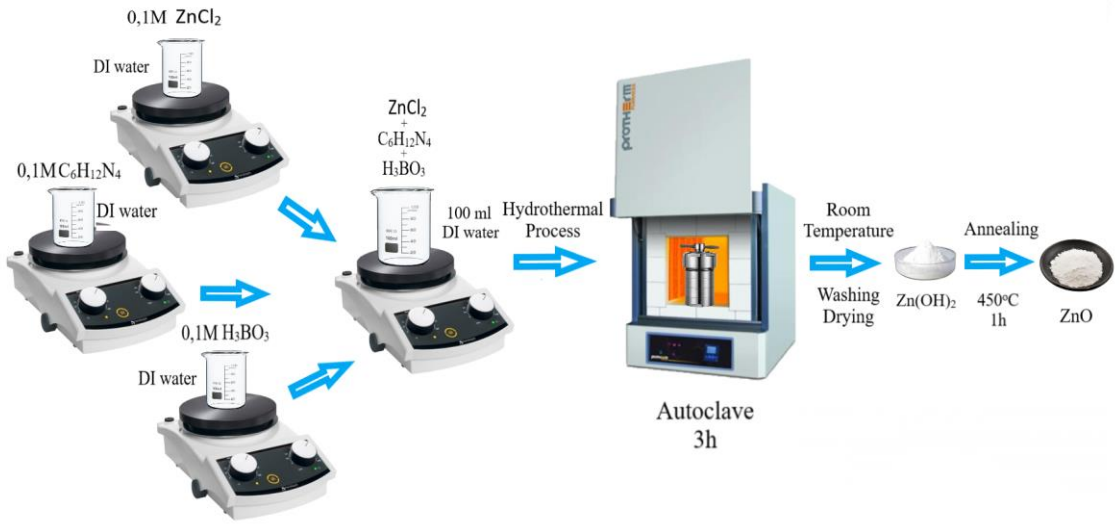

Fig. 1. The steps used in the synthesis of the RGO/ZnO: B composite material.

2.4. Preparation of Working Electrodes

Working electrodes were prepared from 70:20:10 weight ratios for the RGO/ZnO: B composite, the graphite powder, and polytetrafluoroethylene (PTFE), respectively. A small amount of butanol was added dropwise to the mixture. Then, the slurry obtained was spread on nickel foam with dimensions of 1 cm × 1 cm and dried at room temperature for 24 hours. All experiments were conducted using Iviumstat potentiostat/ galvanostatic cyclic voltammetry. To measure the electrochemical characteristics of the working electrodes a typical three-electrode cell was used with a working electrode (Graphite / PTFE / RGO /ZnO: B composite), counter electrode (platinum foil), and reference electrode (standard calomel electrode or SCE). All electrochemical measurements took place in 6 M of KOH (potassium hydroxide) solution as the electrolyte. In the characterization, the XRD pattern was constructed using a Philips X'Pert PRO device. Raman measurements were conducted using a portable Raman spectrometer (BWS465, B&W Tek Inc.) with a 3 cm^{-1} resolution, at a wavelength of 785 nm using a 302 mW diode laser, and SEM images were obtained using a Zeiss EVO 10LS device. The analyses were carried out in the laboratory of Kahramanmaras Sütcü Imam University ÜSKİM (University-Industry-State Cooperation Centre).

3. RESULTS AND DISCUSSION

Figs. 2a and 2b present respectively the Raman spectrum and SEM image of the graphene oxide (GO) produced. The D band at a wavelength of 1354 cm^{-1} and the G band at 1602 cm^{-1} can be seen in the Raman spectrum. The presence of the D peak in the spectrum indicates that the oxygen-containing functional groups of GO produced by the Hummers' method caused significant damage to the graphite crystal structure, while the G peak is related to the double degenerate phonon mode in the Brillouin region. This band was formed owing to the vibrations of the sp2 carbon atoms in plane [41]. The scanning electron microscope (SEM) image of GO shows the 2-dimensional GO layers with planar folding. This is because of the oxygen-containing functional groups formed in the process of GO formation and structural defects [42].

As seen from the SEM images, the morphological structures of the RGO/ZnO: B composite materials obtained consist of hexagonal plate and hexagonal rod mixtures (Figs. 3a-e). The distribution of ZnO: B particles between the RGO layers is due to the inability of the graphene layer to be completely reduced and because of the bonding of the remaining oxygen atoms and ZnO: B particles between the layers. In previous studies, it has been found that boron doping reduces the size of ZnO particles [43]. The smaller the particle size, the more particles and voids per unit area, thus allowing the particles to form a larger specific surface area. This is important in terms of increasing the capacitance values of the supercapacitors obtained. The structure of the RGO/ZnO: B composite materials

[DOI: 10.22068/ijmse.3306]

was characterized as a wurtzite ZnO phase (PDF-2, reference code: 01-079-2205), a simonkolleite ($Zn_5(OH)_8Cl_2.H_2O$) zinc hydroxide phase (PDF-2: reference code:00-076-0922) and RGO phase mixtures from the XRD spectrum (Fig. 3f). As seen in the XRD spectrum, besides the peaks belonging to the zinc oxide and zinc hydroxide phases, the relatively weak (002) plane of RGO at $2\theta = 25.7°$ can be seen. The reason for the formation of a hydroxide structure in the complex is the rehydration of the ZnO: B particles and their transformation into a simonkolleite structure after their placement in the GO solution that was used while forming the composite material. No peak of boron and boron compounds was observed in the XRD spectrum of the obtained RGO/ZnO: B particles.

The reason for this can be explained by replacing the boron atoms with Zn atoms and entering the ZnO structure. In addition, it was observed that the peak intensity of (001) decreased with the increase of the boron additive. This indicates a decrease in crystal quality. It can be explained as the replacement of boron atoms with Zn atoms, entering the ZnO structure and decreasing depending on the peak density. I group III. element boron is doped with ZnO, lower radius B^{3+} atoms replace higher radius Zn^{2+} atoms and act as donors [44].

The electrochemical properties of the Graphite/PTFE/RGO/ZnO: B electrodes were examined using capacitance, impedance, and charging/discharging curves. The capacitance values of the electrodes were calculated with the $C = Iort/v \times m$ equation using the voltammogram curve.

The cyclic voltammogram results of the Graphite/PTFE/RGO/ZnO: B electrodes under a 5 mV/s scanning rate in a 6M KOH solution are shown in Fig. 4a. While the CV curves obtained had a rectangular-like structure, those that produced RGO/ZnO: B electrodes did not have redox peaks, but low-intensity redox peaks were still observed in the 10%, 15% and 20% boron reinforced Graphite / PTFE / RGO / ZnO:B electrodes. As seen from the CV curves, the area under the CV curve for all electrodes increased with the addition of boron. In other words, the capacitive performance of RGO/ZnO: B composite electrodes, obtained as a result of doping ZnO with boron, increased. Moreover, the increase in the capacitive performance was directly dependent on the amount of boron. The addition of boron to the crystal structure increases the electrical conductivity, thus enabling a more effective transfer of electrons and charged ions. Due to the extremely small capacitance value of Ni foam, which is used as a substrate in electrode construction, CV measurements of Ni foam are not shown in the graphs. The specific capacitance values of the Graphite / PTFE / RGO / ZnO:B composite material produced from calculated from the CV curves shown in Fig. 4a. are shown in Table 1. As can be seen from this table, the increase in boron doping increased capacitance values.

Nyquist graphs showing the electrochemical impedance values of the electrodes produced from the Graphite/PTFE/RGO/ZnO: B composite material are shown in Fig. 4b. The impedance measurements were conducted over a range from 0.01 Hz to 100 KHz.

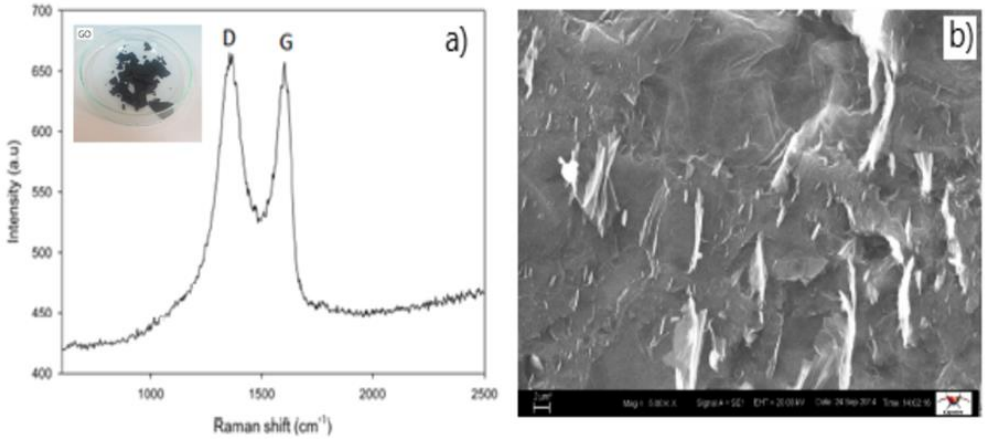

Fig. 2. a) The Raman spectrum and b) SEM image of the graphene oxide (GO).

[DOI: 10.22068/ijmse.3306]

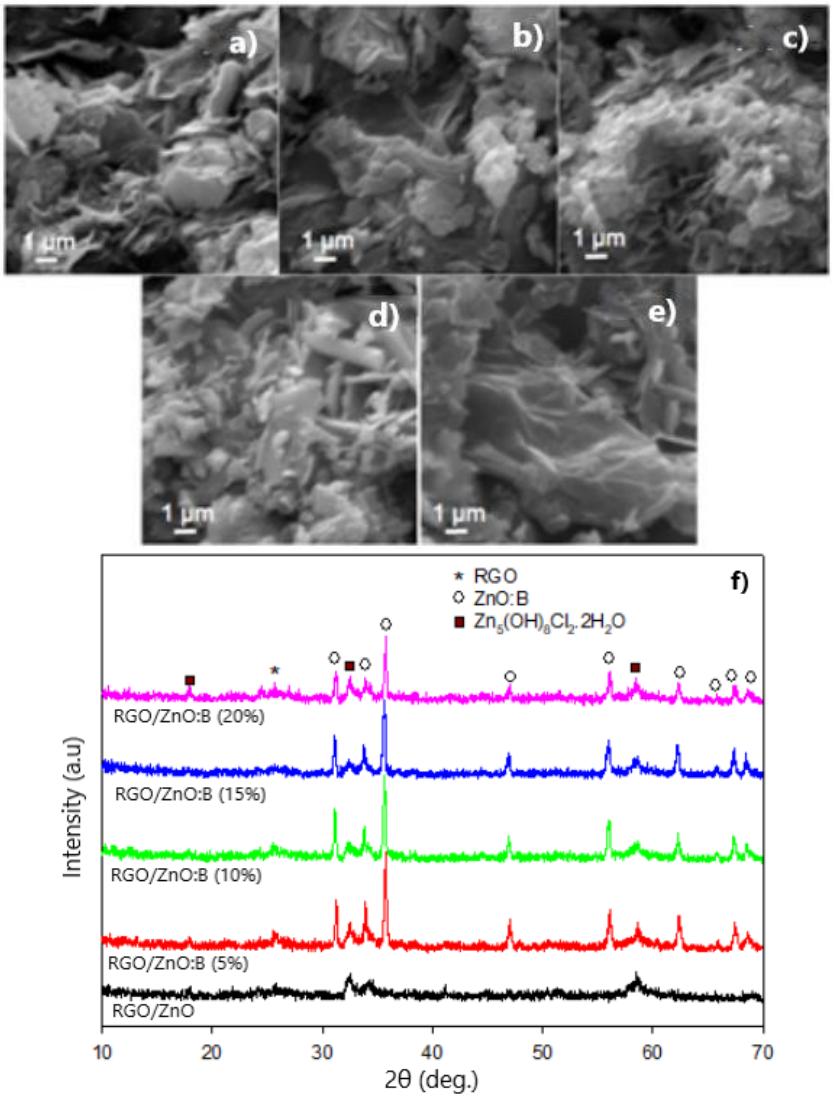

Fig. 3. SEM images of RGO/ZnO:B composites with different boron concentrations: a) 0 wt.% b) 5 wt.% c) 10 wt.% d) 15 wt.% e) 20 wt.% and f) XRD pattern of RGO/ZnO:B composites with different boron concentrations.

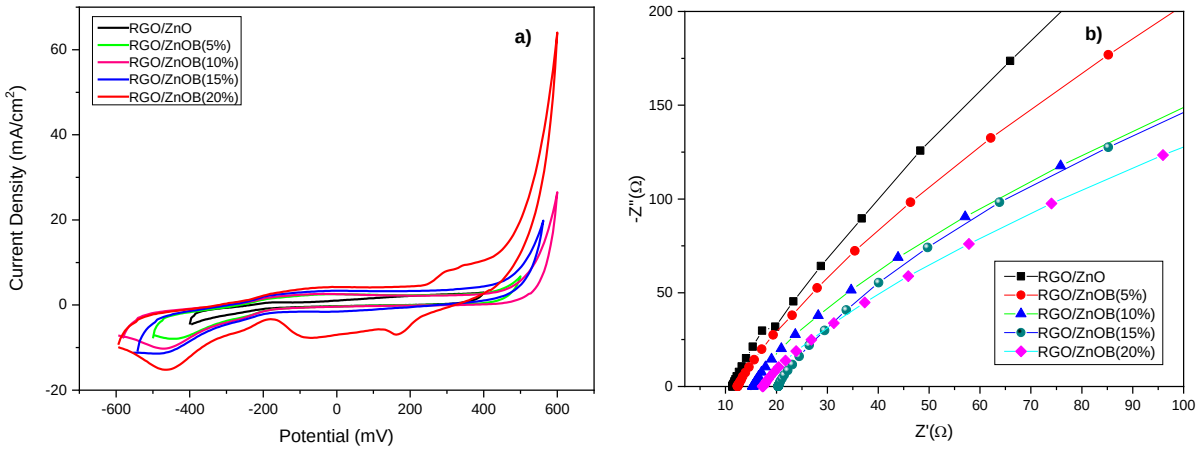

Fig. 4. (a)The cyclic voltammogram graphic and (b) Nyquist impedance spectrum of the Graphite/PTFE/RGO/ZnO:B electrodes under a 5 mV/s scanning rate

[DOI: 10.22068/ijmse.3306]

Table 1. The capacitance values of Graphite/PTFE/RGO/ZnO:B electrodes calculated under a 5 mV/s scanning rate.

$ZnCl_2$	Mean current (mA)	Scanning rate (mV/s)	Capacitance (F/g)	The capacitance decay rate (%) after 100 cycles
RGO/ZnO	2.8	5	36.37	59
RGO/ZnO:B (5% B)	4.9	5	67.12	38
RGO/ZnO:B (10% B)	5.8	5	74.39	46
RGO/ZnO:B (15% B)	7.1	5	79.78	39
RGO/ZnO:B (20% B)	10.6	5	155.88	21

At high frequencies, the intersection point with the real axis (x-axis) in the Nyquist graphic gives the equivalent series resistance (ESR) of the electrode 43,44. The equivalent series resistance includes the resistances of the electrolyte liquid (KOH), the electrode resistance (Graphite / PTFE / RGO / ZnO:B), and the contact resistance of the electrode and current-carrying wires.

The ESR values for the 0%, 5%, 10%, 15%, and 20% boron-reinforced RGO/ZnO electrodes, which are shown in the Nyquist graphics in this figure, were 11.3, 12.2, 15.3, 20.5 and 17.2 Ω, respectively. No significant change was observed in the ESR values of Graphite/PTFE/RGO/ZnO: B electrodes under boron doping, but there were slight increases. In general, it can be said that the boron additive, albeit small, provides better ionic conductivity. No semi-circular curve was encountered in the low-frequency region of the impedance measurements that would have indicated resistance to the charge transfer on the electrode interface. This state indicates the rapid charge transfer at the electrode–electrolyte interface.

Fig. 5a illustrates the electrical charge–discharge curves of the electrodes produced from RGO/ZnO:B composite materials. The measurements were done under a constant 1.2 mA current and between 0 and 0.65 volts. As can be seen from the charge–discharge curves, boron doping increases the charge–discharge duration. The charge–discharge curves of the Graphite/PTFE/RGO/ZnO:B electrodes form a rectangular structure. The nonlinear shapes of the charge-discharge curves confirm the pseudo-capacitance behavior of metal oxides at the electrode/electrolyte interface due to electrochemical adsorption-desorption or redox reaction. The linear portions of the discharge curves show the double-layer capacitance behavior of the electrodes due to charge separation between the electrode/electrolyte interfaces. From the charge-discharge curves of the electrodes, it was observed that boron additive accelerated the filling time and slowed the discharge time. The change in the specific capacitance values of the Graphite/PTFE/RGO/ZnO:B electrodes depend on the changes in scanning rate as shown in Fig. 5b. For all electrodes, the scanning rates were selected to be 5, 10, 50, and 100 mV/s, and in all of them the capacitance values declined with increasing scanning rates. The stability tests of Graphite/PTFE/RGO/ZnO:B electrodes under a 5 mV/s scanning rate are shown in Fig. 5c. The capacitance values of the produced electrodes were computed after running 100 cycles, and at the end of these cycles the decreases in the capacitance value as a percentage are given in Table 1. As can be seen in the values listed in Table 1, the changes in the capacitance values of the boron-reinforced electrodes after 100 cycles are quite low compared to the ones without boron doping. These results indicated that boron-reinforced Graphite/PTFE/RGO/ZnO electrodes have extended durability.

The systematic increase in the capacitance values of the RGO/ZnO: B electrodes as a result of boron doping can be seen in Fig. 6.

4. CONCLUSIONS

In this study, the RGO-embedded, boron-reinforced, composite ZnO materials were successfully synthesized via the hydrothermal method. The supercapacitor electrodes were crafted from the resulting materials and these electrodes were examined to see how their capacitance values changed according to their boron doping concentration.

The structural and morphological characterization of the RGO/ZnO:B composites illustrated that the ZnO:B particles were dispersed in between the RGO sheets as hexagonal rods (Figs. 3a-e).

[DOI: 10.22068/ijmse.3306]

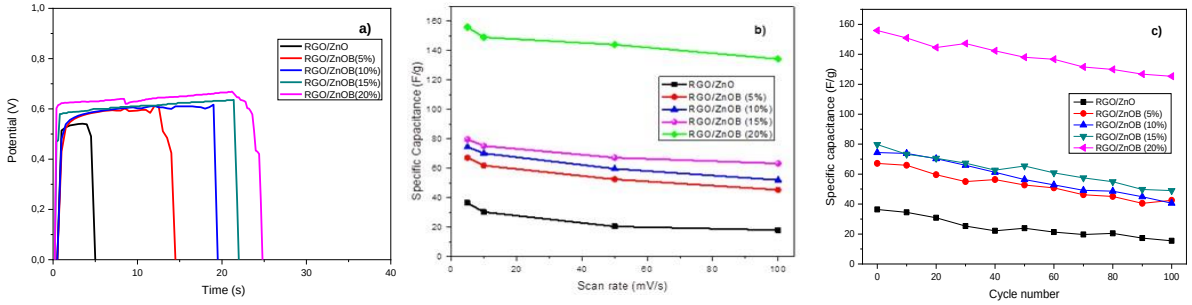

Fig. 5. a) The charge/discharge curves of Graphite/PTFE/ RGO/ZnO:B electrodes b) The changes in capacitance value under different scanning rates, and c) The changes in capacitance values according to the number of cycles.

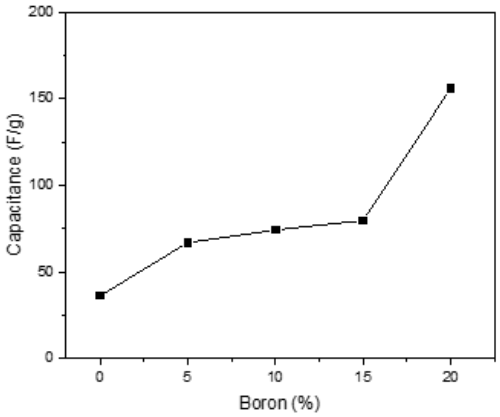

Fig. 6. The changes in the capacitance values of the Graphite/PTFE/RGO/ZnO:B electrodes under a 5 mV/s scanning rate according to the amount of boron.

Supercapacitor electrodes were obtained by spreading the paste – composed of RGO/ZnO: B + graphite + polytetrafluoroethylene (PTFE) and butanol – on Ni foam with dimensions of 1 cm × 1 cm. At the end of the electrochemical analyses, it was observed that increasing boron concentration also increased the capacitance values. The specific capacitance value of the 20% reinforced Graphite / PTFE / RGO / ZnO:B composite electrode was 155.88 F/g, while that of the Graphite / PTFE / RGO / ZnO composite electrode was 36.37 F/g. According to this result, the performance of the capacitance increased four-fold with a 20% boron concentration. Moreover, longer cycle performance of the Graphite / PTFE / RGO / ZnO:B electrodes with higher boron concentration was observed. The capacitance decay (capacitance reduction) of Graphite / PTFE / RGO / ZnO:B electrodes after 100 cycles were lower in electrodes with higher boron concentration. In other words, electrodes with a high boron concentration display a longer duration cycle performance.

ACKNOWLEDGEMENT

This work was supported by the Scientific and Technological Research Council of Turkey, TUBITAK (Grants No: 113F044).

REFERENCES

[1]. Winter, M. and Brodd, R. J., ‟ What are Batteries, Fuel Cells, and Supercapacitors?″ Chem. Rev., 2004, 104, 4245-4269.

[2]. Jose, J., Thomas, V., Vinod, V., Abraham, R. and Abraham, S., ‟ Nanocellulose Based Functional Materials for Supercapacitor Applications.″ J. Sci. Adv. Mater. Devices., 2019, 4, 333-340.

[3]. Vinodh, R., Gopi C. V. V. M., Kummara V. G. R., Atchudan R., Ahamad T., Sambasivam S., Yi M., Obaidat I. M. and Kim HJ., ‟ A Review on Porous Carbon Electrode Material Derived from Hyper Cross-Linked Polymers for Supercapacitor Applications.″ J. Energy Storage., 2020, 32, 101831(1-20).

[DOI: 10.22068/ijmse.3306]

[4]. Yan, J., Liu, T., Liu, X., Yan, Y. and Huang, Y., ″ Metal-Organic Framework-Based Materials for Flexible Supercapacitor Application.″ Coord. Chem. Rev., 2022, 452, 214300 (1-29).

[5]. Nandi, D., Mohan, V. B., Bhowmick, A. K. and Bhattacharyya, D., ″ Metal/Metal Oxide Decorated Graphene Synthesis and Application as Supercapacitor: A Review." J. Mater. Sci., 2020, 55, 6375-6400.

[6]. Wang, H., Casalongue, H. S., Liang, Y. and Dai, H., ″ $Ni(OH)_2$ Nanoplates Grown on Graphene as Advanced Electrochemical Pseudocapacitor Materials." J. Am. Chem. Soc., 2010, 132, 7472-7477.

[7]. Azwar, E., Mahari, W. A. W., Chuah, J. H., Vo D. V. N., Ma N. L., Lam W. H. and Lam S. S., ″ Transformation of Biomass into Carbon Nanofiber for Supercapacitor Application – A Review." Int. J. Hydrogen Energy., 2018, 43, 20811-20821.

[8]. Cui, M., and Meng, X., ″ Overview of Transition Metal-Based Composite Materials for Supercapacitor Electrodes." Nanoscale Adv., 2020, 2, 5516-5528.

[9]. Zhai, Y., Dou Y., Zhao D., Fulvio P. F., Mayes R. T. and Sheng Dai S., ″ Carbon Materials for Chemical Capacitive Energy Storage." Adv. Mater, 2011, 23, 4828-4850.

[10]. Bhujel, R., Rai, S., Deka, U. and Swain, B. P., ″ Electrochemical, Bonding Network and Electrical Properties of Reduced Graphene Oxide-Fe_2O_3 Nanocomposite for Supercapacitor Electrodes Applications." J. Alloys Compd., 2019, 792, 250-259.

[11]. Ke, Q. and Wang, J., ″ Graphene-Based Materials for Supercapacitor Electrodes – A Review." J. Mater., 2016, 2, 37-54.

[12]. Sahoo, R., Lee, T. H., Pham, D. T., Luu, T. H. T. and Lee, Y. H., ″ Fast-Charging High-Energy Battery-Supercapacitor Hybrid: Anodic Reduced Graphene Oxide-Vanadium(IV) Oxide Sheet-on-Sheet Heterostructure." ACS Nano., 2019, 13, 10776-10786.

[13]. Toufani, M., Kasap, S., Tufani A., Bakan F., Weber S., and E Erdem E., ″ Synergy of Nano-ZnO and 3D-Graphene Foam Electrodes for Asymmetric Supercapacitor Devices." Nanoscale., 2020, 12, 12790-12800.

[14]. Wang, Z., Gao, H., Zhang, Q., Liu, Y., Chen, J. and Guo Z., ″ Recent Advances in 3D Graphene Architectures and Their Composites for Energy Storage Applications". Small., 2019, 15, 1-21.

[15]. Xu, H., Ma, L. and Jin, Z., ″ Nitrogen-Doped Graphene: Synthesis, Characterizations and Energy Applications." J. Energy Chem., 2018, 27, 146-160.

[16]. Raj, H., Sil, A. and Pulagara, N. V., ″ MnO Anchored Reduced Graphene Oxide Nanocomposite for High Energy Applications of Li-ion Batteries: The Insight of the Charge-Discharge Process." Ceram. Int., 2019, 45, 14829-14841.

[17]. Nagaraju, P., Alsalme, A., Alswieleh, A. and Jayavel, R., ″ Facile In-situ Microwave Irradiation Synthesis of TiO_2/Graphene Nanocomposite for High-Performance Supercapacitor Applications." J. Electroanal. Chem., 2018, 808, 90-100.

[18]. Mahmoudi, T., Wang, Y. and Hahn, Y. B., ″ Graphene and Its Derivatives for Solar Cells Application." Nano Energy., 2018, 47, 51-65.

[19]. Kumar, R., Sumanta Sahoo, S., Joanni, E., Singh, R. K., Yadav, R. M., Verma R. K., Singh, D. P., Tan, W. K., Pino, A. P., Moshkalev, S. A. and Atsunori Matsuda, A., ″ A Review on Synthesis of Graphene, h-BN, and MoS_2 for Energy Storage Applications: Recent Progress and Perspectives." Nano Res., 2019, 12, 2655-2694.

[20]. Huang, A., He, Y., Zhou, Y., Zhou, Y., Yang, Y., Zhang, J., Luo, L., Mao, Q., Hou, D., and Yang, J., ″ A Review of Recent Applications of Porous Metals and Metal Oxide in Energy Storage, Sensing, and Catalysis." J. Mater. Sci., 2019, 54, 949-973.

[21]. Li, Y., Xu, Y., Yang, W., Shen, W., Xue, H. and Pang, H., ″ MOF-Derived Metal Oxide Composites for Advanced Electrochemical Energy Storage". Small., 2018, 14, 1-24.

[22]. Sethi, M., Shenoy, U. S. and Bhat, D. K., ″ Simple Solvothermal Synthesis of Porous Graphene-NiO Nanocomposites with High Cyclic Stability for Supercapacitor Application." J. Alloys Compd., 2021, 854, 157190 (1-10).

[DOI: 10.22068/ijmse.3306]

[23]. Li, S., Li, S., Jiang, H., Yang, K., Zhang, Z., Li, S., Luo, N., Liu, Q., Ran Wei, R., " Three-Dimensional Hierarchical Graphene/TiO_2 Composite as a High-Performance Electrode for Supercapacitor." J. Alloys Compd. 2018, 746, 670-676.

[24]. Lv, H., Yuan, Y., Xu, Q., Liu, H., Wang, Y. G., Xia, Y., " Carbon Quantum Dots Anchoring MnO_2/Graphene Aerogel Exhibits Excellent Performance as Electrode Materials for Supercapacitor." J. Power Sources., 2018, 398, 167-174.

[25]. Kumar, R., Youssry, S. M., Soe, H. M., Abdel-Galeil, M. M., Kawamura, G. and Matsuda, A., " Honeycomb-Like Open-Edged Reduced-Graphene-Oxide-Enclosed Transition Metal Oxides (NiO/Co_3O_4) as Improved Electrode Materials for High-Performance Supercapacitor." J. Energy Storage., 2020, 30, 101539 (1-12).

[26]. Obodo, R. M., Nwanya, A. C., Arshad, M., Iroegbu, C., Ahmad, I., Osuji, R. U., Maaza, M. and Ezema, F. I., " Conjugated NiO-ZnO/GO Nanocomposite Powder for Applications in Supercapacitor Electrodes Material." Int. J. Energy Res., 2020, 44, 3192-3202.

[27]. Giampiccolo, A., Tobaldi, D. M., Leonardi, S. G., Murdoch, B. J., Seabra, M. P., Ansella, M. P., Neri, G. and Ball R. J., " Sol-gel Graphene/TiO_2 Nanoparticles for the Photocatalytic-Assisted Sensing and Abatement of NO_2." Appl. Catal. B Environ., 2019, 243, 183-194.

[28]. Phongprueksathat, N., Bansode, A., Toyao, T. and Urakawa, A., " Greener and Facile Synthesis of Cu/ZnO Catalysts for CO_2 Hydrogenation to Methanol by Urea Hydrolysis of Acetates." RSC Adv., 2021, 11, 14323-14333.

[29]. Mandhare, H., P. Barai, D., A. Bhanvase, B. and Saharan, V. K., " Preparation and Thermal Conductivity Investigation of Reduced Graphene Oxide-ZnO Nanocomposite-Based Nanofluid Synthesized by the Ultrasound-Assisted Method." Mater. Res. Innov., 2020, 24, 433-444.

[30]. Yu, Y., Mottaghi-Tabar, S., Iqbal, M. W., Yu, A. and Simakov, D. S. A., " CO_2 Methanation Over Alumina-Supported Cobalt Oxide and Carbide Synthesized by Reverse Microemulsion Method." Catal. Today, 2022, 379, 250-261.

[31]. Mughal, A. S., Zawar, S., Ansar, M. T., Nafzal, F., Murtaza, G., Atiq, S. and Ramay, S. M., " Efficient Electrochemical Performance of Hydrothermally Synthesized Mixed Transition Metal Oxide Nanostructures." Ionics (Kiel)., 2022, 28, 2469-2479.

[32]. Paraschiv, C., Hristea, G., Iordoc, M., Sbarcea, B. G. and Marinescu, V., " Hydrothermal Growth of ZnO/GO Hybrid as an Efficient Electrode Material for Supercapacitor Applications". Scr. Mater., 2021, 195, 113708 (1-5).

[33]. Nagaraju, Y. S., Ganesh, H., Veeresh, S., Vijeth, H., Basappa, M. and Devendrappa, H., " Self-Templated One-step Hydrothermal Synthesis of Hierarchical Actinomorphic Flower-like SnO_2-ZnO Nanorods for High-Performance Supercapacitor Application." J. Electroanal. Chem., 2021, 900, 1157418(1-10).

[34]. Khudiar, S. S., Mutlak, F. A. H. and Nayef, U. M., " Synthesis of ZnO Nanostructures by Hydrothermal Method Deposited on Porous Silicon for Photo-Conversion Application." Optik., 2021, 247, 167903(1-6).

[35]. Cheng, Q., Tang, J., Ma, J., Zhang, H., Shinya, N. and Qin, L. C., " Graphene and Nanostructured MnO_2 Composite Electrodes for Supercapacitors." Carbon N. Y., 2011, 49, 2917-2925.

[36]. Trinity Rabecca, H. J. and Clement Lourduraj, A. J., " Synthesis of Reduced Graphene Oxide and A Study on Its Electrochemical Performance for Supercapacitor Applications." Mater. Today Proc., 2022, 68, 335-340.

[37]. Paulchamy, B., Arthi, G. and Lignesh B.D., " A Simple Approach to Stepwise Synthesis of Graphene Oxide Nanomaterial". J. Nanomed. Nanotechnol., 2015, 06, 1-4.

[38]. Ghoderao, K. P., Jamble, S. N. and Kale, R. B., " Influence of pH on Hydrothermally Derived ZnO Nanostructures." Optic., 2018, 156, 758-771.

[39]. Jang, J. M., Kim, S. D., Choi, H. M., Kim, J. Y. and Jung, W. G., " Morphology Change of Self-Assembled ZnO 3D

[DOI: 10.22068/ijmse.3306]

Nanostructures with Different pH in the Simple Hydrothermal Process." Mater. Chem. Phys., 2009, 113, 389-394.

[40]. Das, R., Kumar, A., Kumar, Y., Sen, S. and Shirage, P. M., " Effect of Growth Temperature on the Optical Properties of ZnO Nanostructures Grown by Simple Hydrothermal Method."RSC Adv., 2015, 5, 60365-60372.

[41]. Mei, X., Meng, X. and Wu, F., " Hydrothermal Method for the Production of Reduced Graphene Oxide." Phys. E Low-Dimensional Syst. Nanostructures., 2015, 68, 81-86.

[42]. Ramanathan, Abdala, A. A., Stankovich, S., Dikin, D. A., Herrera-Alonso, M., Piner, R. D., Adamson, D. H., Schniepp, H. C., Chen, X., Ruoff, R. S., Nguyen, S. T., Aksay, I. A., Prud'Homme, R. K., and Brinson, L. C., " Functionalized Graphene Sheets for Polymer Nanocomposites." Nat. Nanotechnol., 2008, 3, 327-331.

[43]. Senol, S. D., Ozturk, O., and Terzioğlu, C., " Effect of Boron Doping on the Structural, Optical and Electrical Properties of ZnO Nanoparticles Produced by the Hydrothermal Method". Ceramics International., 2015, 41(9), 11194-11201.

[44]. Gomathisankar, P., Hachisuka, K., Katsumata, H., Suzuki, T., Funasaka, K,. and Kaneco, S., " Photocatalytic Hydrogen Production from Aqueous Na_2S + Na_2SO_3 Solution with B‐Doped ZnO."ACS Sustainable Chem. Eng., 2013 (1), 982-988.

[45]. Gholivand, M. B., Heydari, H., Abdolmaleki, A. and Hosseini, H., " Nanostructured CuO/PANI Composite as Supercapacitor Electrode Material." Mater. Sci. Semicond. Process., 2015, 30, 157-161.

[46]. Jayachandiran, J., Yesuraj, J., Arivanandhan, M., Raja, A., Austin Suthanthiraraj, S., Jayavel, R. and Nedumaran, D., " Synthesis and Electrochemical Studies of rGO/ZnO Nanocomposite for Supercapacitor Application". J. Inorg. Organomet. Polym. Mater., 2018, 28, 2046-2055.

[DOI: 10.22068/ijmse.3306]